Korean Chem. Eng. Res., 61(2), 328-339 (2023)
https://doi.org/10.9713/kcer.2023.61.2.328
PISSN 0304-128X, EISSN 2233-9558

Performance of Cu-SiO_2 Aerogel Catalyst in Methanol Steam Reforming: Modeling of hydrogen production using Response Surface Methodology and Artificial Neuron Networks

Taher Yousefi Amiri*, Mahdi Maleki-Kakelar*,† and Abbas Aghaeinejad-Meybodi**

**Department of Chemical Engineering, University of Zanjan, Zanjan, Iran*
***Department of Chemical Engineering, Urmia University, Urmia, Iran*
(Received 14 May 2022; Received in revised from 26 August 2022; Accepted 16 December 2022)

Abstract – Methanol steam reforming (MSR) is a promising method for hydrogen supplying as a critical step in hydrogen fuel cell commercialization in mobile applications. Modelling and understanding of the reactor behavior is an attractive research field to develop an efficient reformer. Three-layer feed-forward artificial neural network (ANN) and Box-Behnken design (BBD) were used to modelling of MSR process using the Cu-SiO_2 aerogel catalyst. Furthermore, impacts of the basic operational variables and their mutual interactions were studied. The results showed that the most affecting parameters were the reaction temperature (56%) and its quadratic term (20.5%). In addition, it was also found that the interaction between temperature and Steam/Methanol ratio is important on the MSR performance. These models precisely predict MSR performance and have great agreement with experimental results. However, on the basis of statistical criteria the ANN technique showed the greater modelling ability as compared with statistical BBD approach.

Key words: Artificial neural network, Box-Behnken design, Methanol steam reforming, Modelling, Cu-SiO_2 aerogel catalyst

1. Introduction

The hydrogen fuel cell is a promising power supply system in mobile applications instead of traditional energy sources due to its minimal environmental impact, high energy efficiency without Carnot limitation, and no moving parts and noise [1-5]. Hydrogen is the cleanest as well as the most efficient energy source and its combustion in fuel cells produces water as only product [6-10]. However, it is inflammable, explosive in gaseous form, directly unavailable in natural resources with low volume energy density that lead to challenges in safe and economic transport, storage and distribution of hydrogen [1,2,11-13]. Among the different ways to hydrogen supply, online hydrogen production through methanol steam reforming is one of the most promising options [1,4,7,9,11,12,14,15].

Methanol is widely available and produced in large scales using different sources, such natural gas and coal [8,14]. It can be also produced from various renewable sources that lead to sustainable closed circuit [8,12,13,15]. The hydrogen-to-carbon ratio is high in methanol and there is no C-C bond in its formula. It can be straightforwardly reformed at lower temperatures with higher hydrogen yield than many other hydrocarbon fuels, minimal coke formation on the catalysts as well as no NOx and SOx emissions [6-8,12,14-16,19, 20].

Overall methanol steam reforming reaction as shown in Eq. 1 excluding CO production. However, reverse water-gas shift (RWGS) and methanol decomposition (MD) reactions take place during methanol reforming, which leads to CO formation in the reformer [8,16]. Lowering the reforming temperature reduces the CO formation through MD or RWGS, but it is not kinetically desirable because it reduces the hydrogen yield and increases the reformer volume [7,8,16]. Also, catalyst deactivation as a result of sintering or coke deposition will be suppressed at lower temperatures [7]. Therefore, to enhance the reformer compactness and performance, which is an imperative requisite in mobile applications [21], some solutions have been proposed such as micro-reactors, membrane reactors as well as attempts to prepare more active catalysts. However, high cost and complex fabrication methods of membrane reactors and micro-reactors limit their entrance to the market. Fixed bed reactors thus have simple and mature technology and are still the main option for MSR [20]. Accordingly, catalyst activity, selectivity and stability are the key issues for the MSR technology success for hydrogen supplying in mobile applications [8-10,19].

$$\text{MSR: } CH_3OH + H_2O \rightarrow 3H_2 + CO_2 \quad (1)$$
$$\text{MD: } CH_3OH \rightarrow 2H_2 + CO \quad (2)$$
$$\text{RWGS: } CO_2 + H_2 \rightarrow H_2O + CO \quad (3)$$

In general, Cu and Pd are the main catalyst components for the MSR process. Cu-based catalysts have the highest activity and selectivity in MSR reaction, and Cu/ZnO/Al_2O_3 has been widely used for this reaction [1,6-8]. However, traditional copper catalysts have poor Cu dispersion and high susceptibility to sintering at high

† To whom correspondence should be addressed.
E-mail: mmaleki@znu.ac.ir

temperatures and thermal instability [1,8,19]. Despite the higher thermal stability of Pd catalysts, their higher cost and selectivity to CO formation limit their application [8,20,24]. Therefore, many researchers have attempted to develop alternative catalyst systems for improving the catalyst characteristics and performance by addition of different promoters, dopants or by changing the supports or synthesis methods [1,19]. Among the different studied catalyst systems, the high performance of Cu-SiO_2 catalyst in MSR has been proven [10,25-27]. Nature of support, its porosity and surface area, and synthesis method could significantly affect the dispersion and particle sizes of the active metals, interaction between catalytic metals and support and consequently the catalyst activity [6,12,28]. Silica aerogel has been utilized as efficient catalyst support due to its high surface area, excellent pore volume, desired pore size distribution and interconnected pores. Good characteristics and performance of copper-silica aerogel catalyst in MSR process have been demonstrated in our previous work [29-32].

Alternatively, it will be possible optimizing the reactor condition by understanding the operating parameters effects on the MSR performance in order to provide an efficient reformer. Several researchers have attempted experimentally or theoretically to find how the operating parameters influence the methanol conversion, hydrogen yield and CO selectivity [18,22,33]. Although the conventional 'one-variable-at-a-time' (OVAT) strategy may be easy to operate and analyze, this approach frequently disregards the interactions among influential factors. Furthermore, the performance evaluation by using OVAT is both time consuming and expensive [34].

Conversely, the statistical approaches, such as response surface methodology (RSM), include not only carefully picking out a small number of experiments that are to be performed under controlled situations, but also organizing the conducting of the experiment under statistically optimal conditions [35]. The RSM, which was first introduced by Box and Wilson (1951), has been an effective tool to improve the performance of processes in the chemical industry. As a practical kind of this methodology, Box-Behnken design (BBD) can statistically model the influence of the operating parameters, both separately and as their cumulative interactions, on the system output. The estimation of the quadratic model parameters, constructing sequential designs and detection of lack of fit of the model makes BBD a suitable option among the techniques of response surface methodology for many chemical processes [4,8,36]. However, BBD similar to other response surface designs is exact for only a narrow range of input process parameters, and consequently their applications are practically restricted to typically non-linear processes.

As an encouraging alternative modeling technique, artificial neural network (ANN) has recently been applied in multivariate non-linear processes for constructing rigorous models. The fundamental computational structures of an ANN are analogous to the nervous systems function of the human brain. It can be applied for assessing a non-linearity between the influential factors and responses through iterative training of data attained from a design of experiments. Superior features of ANNs over conventional methods in modeling and forecasting, such as tolerance patterns, universal approximation capability and no need for system model, have made them popular tools in modeling of many complicated (bio)chemical processes [35, 37-39]. Accordingly, ANNs have been applied so far to deal with a variety of problems, for instance modeling intricate process [40], describing the nonlinear relationship between input and output variables [41].

To the best of our knowledge, there are limited studies on the application of BBD and ANN for modelling hydrogen production through methanol steam reforming. Hence, our prime research objective set out to investigate the effects and interaction effects of influential variables on performance of Cu-SiO_2 aerogel catalyst in methanol steam reforming via modeling and experimental evaluation. In this respect, particular focus is on the application of RSM based BBD approach to acquire a quadratic polynomial model and predict the amount of methanol conversion. Then, the BBD results are in comparison to ANN predictions with the aim of attaining the best modeling and optimization method for producing the hydrogen through MSR using Cu-SiO_2 aerogel catalyst.

2. Materials and Methods

2-1. Experimental setup

Cu-SiO_2 aerogel catalyst synthesis method was described in detail elsewhere [29,30]. In summary, water solutions of sodium silicate and $Cu(NO_3)_2 \cdot 3H_2O$, respectively, as silica and copper precursors were mixed vigorously together. Obtained solution was aged to co-gelation of copper and silica precursors. The formed gel was immersed, respectively, in isopropyl alcohol and hexane to pore solvent exchange solvent and then in 20% HMDZ (Merck) solution in hexane to gel surface modification. Finally, the obtained wet gel is dried in ambient pressure under a programmed temperature up to 120 ℃ copper-silica aerogel, then, calcined to 700 ℃.

Copper content of the used catalyst was 13.3 wt%, which was determined by atomic absorption spectrometry (AAS, Analytic Jena nova 300). Catalytic tests of the Cu-SiO_2 aerogel catalysts were carried out in a U-tube Pyrex reactor (i.d =4 mm). 1.0 gr of Cu-SiO_2 catalyst with 1-2 mm particles sizes was filled inside reactor. Both sides of the catalyst bed were filled with glass beads. The reactor was placed inside an electrical furnace equipped with K-type thermocouple. Furnace (reactor) temperature was controlled using NP100 HANYOUNG controller. The liquid reactants including methanol and water were mixed together in the desired molar ratio and poured into the liquid feed container. During the experiments, the liquid feed was injected into the reactor entrance with the desired flow rate by a syringe pump (702 SM Titrino, Metrohm, with an accuracy of 0.01 ml/min). Argon was used as carrier gas which carries the liquid feed into the reactor. To disturb the feed stream, glass particles were filled before the catalytic bed inside the reactor. The feed stream was heated and evaporated during passing the glass beads before reaching the catalyst

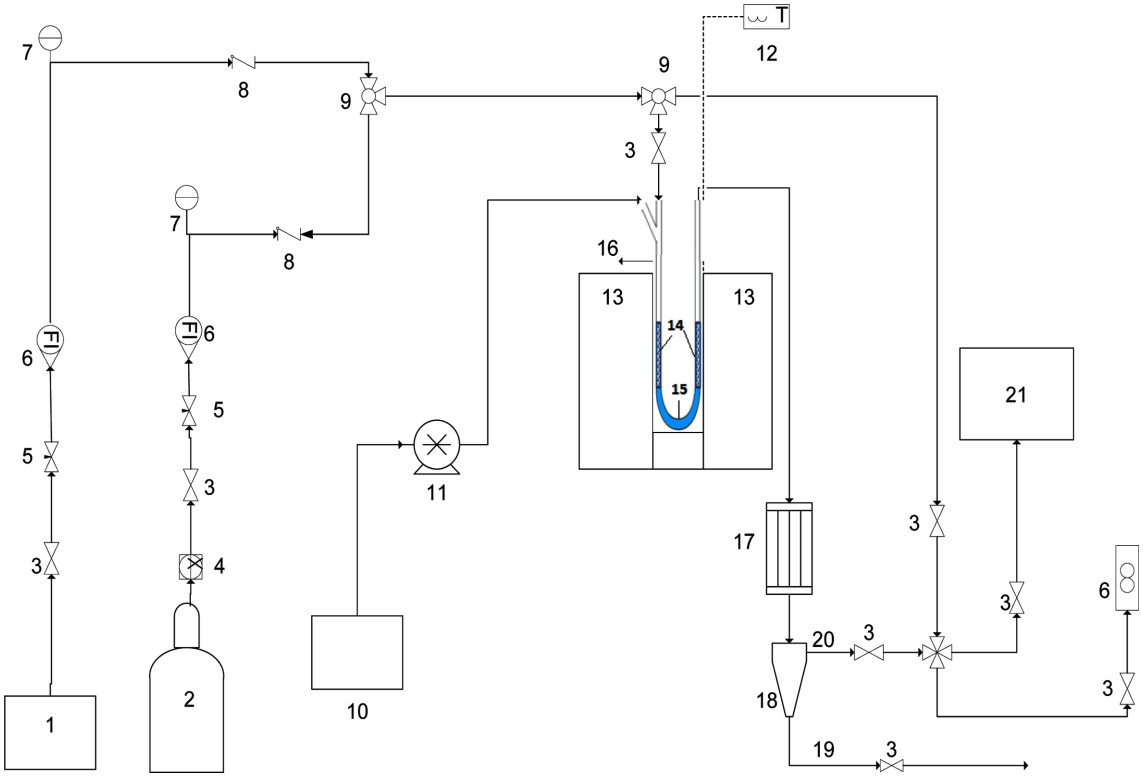

Fig. 1. Schematic view of the experimental setup used for reaction tests.

1. Hydrogen generator
2. Argon cylinder
3. Valve
4. Pressure regulator
5. Needle valve
6. Flow meter
7. Pressure indicator
8. Check valve
9. Three way valve
10: Feed mixture
11. Syringe pump
12. Temperature controller
13. Furnace
14. Glass beads
15. catalyst bed
16: Reactor
17: Condenser
18: Gas – liquid separator
19: Collected liquid
20: Dry product gas
21: Gas chromatograph

bed. Reactor effluent was passed the condenser and the unreacted water and methanol were separated from the product gas. Then, the product gas was analyzed by online gas chromatography (Agilent Technologies7890AGC). HP-Plot/Q capillary column (30 m, 0.53 mm, 40 μm) and TCD detector have been used in GC. Product gas included hydrogen, carbon dioxide and carbon monoxide. A schematic view of the experimental setup is presented in Fig. 1. Methanol conversion was calculated as:

$$\text{Methanol Conversion (\%)} = \frac{(n^P_{CO_2} + n^P_{CO})}{n^F_{CH_3OH}} \times 100 \quad (4)$$

in which n_i is the molar rate of the i component and superscripts of F and P are feed and product streams. H_2 stream at 300 ℃ for 2 h was used for loaded catalyst reduction prior to MSR reaction.

2-2. Experimental design

The experimental design was employed an RSM based BBD (Table 1). The four-factor, three-level BBD was proceeded to optimize the synergistic effect of variables and to find the response pattern. The operating parameters range was found based on preliminary analysis, liquid feed flow rate (1.2~4.8 mL/h), reaction temperature (250~350 ℃), steam/methanol molar ratio (1.2~5) and carrier gas flow (30~80 mL/min) were investigated on the methanol conversion (%).

Table 1. Experimental ranges and levels of the independent test variables

Independent variables	Factor X_i	Ranges and levels		
		Low	Centre	High
Liquid feed flow rate (mL/h)	(X_1)	1.2	3	4.8
Reaction temperature (℃)	(X_2)	250	300	350
Steam/Methanol molar ratio (-)	(X_3)	1.2	3.1	5
Carrier gas flow (mL/min)	(X_4)	30	55	80

Experimental output was calculated to find the optimal level of the factors. The variables were normalized at three levels from −1, 0 and +1 as defined by Eq. (5).

$$x_i = \frac{X_i - X_0}{\Delta X_i} \quad (5)$$

where x_i is input coded variable. The real value of independent variables and its value at the centre point are labelled with X_i and X_0, respectively. ΔX_i is also increment. The results of experiments were statistically analyzed by using Minitab 14 statistical package (MINITAB Inc., PA, USA).

2-3. ANN modelling

A neural network mimics the learning process of the brain through mathematical descriptive model of interconnected nerve cells [35]. The basic forms of neural networks are typically feed forward neural

networks (FFNNs) that include an input layer, an output layer, and one or more hidden layers. According to the required specified architecture, many simple processing elements are interconnected in this type of network, by the weighted connections [42]. The hidden layer, which is linked to the input and output layers by adjustable weights, enables the network to estimate intricate relationships between the input and output variables. Of course, finding the hidden layer neurons is a crucial step which plays a noticeable part in the efficiency of the neural network [43,44]. So as to acquire the optimal neural network, various types of transfer functions in each layer, as well as varied numbers of neurons in hidden layer, were designated. Where two different networks have had the identical performance, the network having fewer neurons was preferred [45].

ANN were developed by optimizing network architecture parameters based on BBD. For this purpose, independent variables were used as inputs to the network, while methanol conversion was used as output of the network.

For prevention of the saturation problems associated with the sigmoid transfer function in the network, all the data (X_i) were transformed to a normalized values (x_i) in a uniform range (0.1 to 0.9) by using the following expression [46]:

$$x_i = 0.1 + \frac{0.8(X_i + \min(X_i))}{\max(X_i) - \min(X_i)} \tag{6}$$

Different criteria, e.g. mean absolute error (MAE) and the mean square error (MSE), were adopted to appraise the performance of constructed models for estimation of the methanol conversion. These criteria were calculated using the following equations:

$$\text{MSE} = \frac{\sum_{i=1}^{n} (\Upsilon_{ANN} - \Upsilon_{Obs})^2}{n} \tag{7}$$

$$\text{MAE} = (1/n) \sum_{i=1}^{n} |\Upsilon_{ANN} - \Upsilon_{Obs}| \tag{8}$$

where i, n, Υ_{Obs} and Υ_{ANN} are the index of data, the numbers of the experimental runs, the observed and the ANN methanol conversion prediction, respectively. All the data were randomly divided into three subsets: training (70% of the data), testing (20% of the data) and validation (10% of the data). All the analyses of issues in connection with the data analysis skills were done through the use of MATLAB v. 8.5.0.197613.

Finally, to analyze the performance of the RSM and ANN models, the ANN and BBD outputs for designing the experiments were plotted against the corresponding experimental data. The much closer to the perfect forecast line, in which the predicted values are equal to the corresponding observed data, the superior the modeling ability of a specified model.

3. Results and Discussion

3-1. BBD modelling

The BBD matrix for 4-factors with 3-levels for methanol conversion are presented in Table 2. So as to match the relationship between the dependent and the independent variables, the following 2nd-order polynomial was fitted to the experimental data designed by BBD.

$$\Upsilon = \beta_0 + \sum_{i=1}^{k} \beta_i \chi_i + \sum_{i=1}^{k} \beta_{ii} \chi_{ii}^2 + \sum_{i=1}^{k-1} \sum_{i=1}^{k} \beta_{ij} \chi_i \chi_j + \varepsilon \qquad i \neq j \tag{9}$$

where Υ and χ stand for the response variable and input variables in coded units, respectively. In this equation, intercept term, linear, quadratic and interaction effects are also labelled with β_0, β_i, β_{ii}, β_{ij}, respectively [47,48]. Furthermore, random error (ε) denotes differences between actual and predicted results. An empirical relationship (Eq. 10) can be established between the response (Methanol conversion (%)) and the input variables (Liquid feed flow rate (mL/h), reaction temperature (℃), steam/Methanol molar ratio (-) and carrier gas flow (mL/min)) from experimental results using coded units.

$$\begin{aligned}\Upsilon = {} & 88.333 - 8.5250\chi_1 + 27.8750\chi_2 + 10.4833\chi_3 - 3.2333\chi_4 \\ & - 1.2167\chi_1^2 - 16.8917\chi_2^2 - 0.6458\chi_3^2 - 2.1292\chi_4^2 + 4.7000\chi_1\chi_2 \\ & + 6.3150\chi_1\chi_3 - 2.1000\chi_1\chi_4 - 7.5000\chi_2\chi_3 + 1.2250\chi_2\chi_4 \\ & + 0.9750\chi_3\chi_4\end{aligned} \tag{10}$$

3-2. Analysis of variance (ANOVA)

Table 3 lists the ANOVA results for the methanol reforming experiments. The results display that the square and interaction effects of independent variables as well as linear parameters have the significant effects (P-value < 0.05) on methanol reforming yield.

In general, if the achieved F-value is bigger than F-distribution value, which is tabulated at an alpha level of 0.05 for a specified value of degree of freedom, this indicates that the BBD is estimating the experimental data well. On the basis of ANOVA table, the attained F-value, specifically 65.94, is apparently greater than the obtained F-distribution (2.637 at 95% significance) demonstrating the effectiveness of the model's fit on the experimental results prediction [49].

According to the P-value for the lack-of-fit tests, i.e., 0.217, the data variation around the fitted model is not significant with regard to the pure error and consequently suggests that the model adequately fits the data [50]. For linear, quadratic and interaction effects of the variables, the estimated regression coefficients, t-value, and P-value are summarized in Table 4, at 95% significance level. The P-value, as well as F-value, was utilized for verification of the statistical significance of each model term.

All four independent variables, second-order effect of reaction temperature, are statistically significant model terms on methanol conversion (P-value < 0.05). Furthermore, interaction effects of liquid feed flow rate and steam/methanol molar ratio with reaction temperature and steam/methanol molar ratio are also extremely significant.

Taken as a whole, our results highlight that the overall influence of the operating variables on methanol conversion is statistically significant (P-value < 0.05).

For further interpreting the experimental results, the percentage

Table 2. The 4-factors three layered Box-Behnken matrix in addition to the observed and the predicted responses

Run	Type of data	Uncoded Values				Methanol conversion (%)		
		Liquid feed flow rate (mL/h)	Reaction temperature (℃)	Steam/Methanol molar ratio (-)	Carrier gas flow (mL/min)	Experimental data	Predicted	
							RSM	ANN
1	Training	3	300	5	30	99.7	99.59	98.45
2	Training	4.8	300	3.1	80	66	71.13	67.69
3	Training	1.2	350	3.1	55	100	101.93	100.01
4	Training	3	300	1.2	30	77	80.58	79.98
5	Training	3	350	3.1	80	99.3	95.18	98.44
6	Training	1.2	250	3.1	55	53	55.58	57.14
7	Training	3	300	1.2	80	72	72.16	72.72
8	validation	3	300	3.1	55	89	88.33	88.62
9	Training	1.2	300	3.1	80	90	92.38	91.98
10	validation	4.8	300	1.2	55	63	62.38	61.48
11	validation	3	300	3.1	55	90	88.33	88.62
12	Training	1.2	300	3.1	30	99.6	94.65	97.28
13	Training	3	250	1.2	55	29	26.23	29.56
14	Test	4.8	250	3.1	55	31	29.13	29.48
15	Training	3	250	5	55	64	62.20	67.11
16	Training	4.8	300	3.1	30	84	81.80	85.09
17	Validation	3	350	3.1	30	99.4	99.20	99.84
18	Test	1.2	300	5	55	100	100.40	98.90
19	Test	3	250	3.1	80	37	36.98	37.96
20	Training	3	300	3.1	55	86	88.33	88.62
21	Training	3	300	5	80	98.6	95.08	94.53
22	validation	3	350	5	55	100	102.95	100.25
23	Test	4.8	350	3.1	55	96.8	94.28	97.83
24	Training	3	350	1.2	55	95	96.98	97.01
25	Training	3	250	3.1	30	42	45.90	46.82
26	Training	4.8	300	5	55	94	96.10	92.87
27	Training	1.2	300	1.2	55	94.5	92.18	91.59

Table 3. ANOVA results for the methanol reforming experiments

Source of variations	Methanol conversion (%)			
	DF	Mean Square	F-value	P-value
Regression	14	997.59	65.94	0.000
Linear	4	2910.14	192.34	0.000
Square	4	455.57	30.11	0.000
Interaction	6	83.89	5.54	0.006
Residuals Error	12	15.13		
Lack-of-Fit	10	17.29	3.99	0.217
Pure Error	2	4.33		

$R^2 = 0.9872$, $R^2(Adj) = 0.9722$

Table 4. Estimated regression coefficients, t-values and P-values

Terms	Methanol conversion (%)		
	Coefficient	t-value	P-value
β_0	88.3333	39.334	0.000
β_1	-8.5250	-7.592	0.000
β_2	27.8750	24.825	0.000
β_3	10.4833	9.336	0.000
β_4	-3.2333	-2.880	0.014
β_{12}	4.7000	2.417	0.033
β_{13}	6.3750	3.278	0.007
β_{14}	-2.1000	-1.080	0.301
β_{23}	-7.5000	-3.856	0.002
β_{24}	1.2250	0.630	0.541
β_{34}	0.9750	0.501	0.625
β_{11}	-1.2167	-0.722	0.484
β_{22}	-16.8917	-10.029	0.000
β_{33}	0.6458	0.383	0.708
β_{44}	-2.1292	-1.264	0.230

influence of factors on the methanol conversion was individually computed as stated by Pareto analysis (Eq. (11)):

$$P_i = \left(\frac{\beta_i^2}{\sum \beta_i^2}\right) \times 100 \qquad i \neq 0 \tag{11}$$

This analysis indicates that the whole factors are effective on the methanol conversion (Fig. 2). It is found that the temperature (X_2, 56.00%) and its quadratic term (X_2^2, 20.56%) are the dominant parameters in this process. Among the variables, S/M molar ratio (X_3, 7.92%) and flow rate (X_1, 5.24%) create the main effects on the methanol conversion. The most significant mutual interactions are flow rate * S/M molar ratio and Temperature * S/M molar ratio, which influence the dependent variables up to 7%.

For attaining the best model's fit for methanol conversion, the final quadratic RSM model is shown as follows (Eq. 12) by eliminating insignificant values from the applied BBD model (P-value > 0.05).

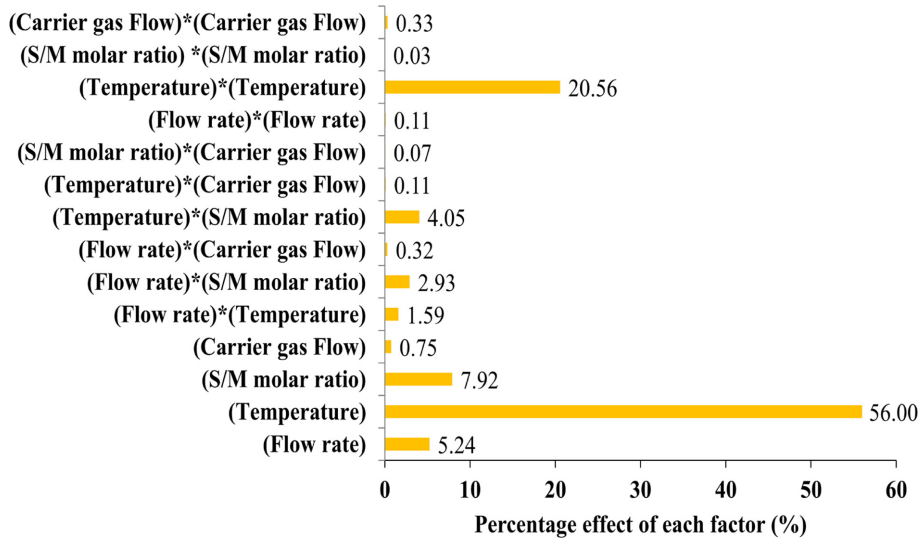

Fig. 2. Pareto graphic analysis.

$$\Upsilon = 88.333 - 8.5250\chi_1 + 27.8750\chi_2 + 10.4833\chi_3 - 3.2333\chi_4 - 16.8917\chi_2^2 + 4.7000\chi_1\chi_2 + 6.3150\chi_1\chi_3 - 7.5000\chi_2\chi_3 \quad (12)$$

3-3. Effect of independent variables

To investigate the mutual interaction between the factors on methanol conversion, 2D contour plots were employed on the basis of the quadratic mathematical statement, whereas 3D response surface plots were utilized to estimate methanol conversion under the applied conditions. Figs. 3-5 illustrate the influence of the independent variables being on the methanol conversion, in the experimental ranges, with the other two variables for each plot held at a constant level.

3-3-1. Effect of liquid feed flow rate and reaction temperature on methanol conversion

As seen in Fig. 3, liquid feed flow has higher effect at lower temperatures. Increasing the temperature supresses the effect of the liquid feed flow rate on the methanol reforming yield. Also, temperature effect at high flow rates is more than its effect at low flow rates. For example, the conversion reduced from 64 to 45% at 250 ℃ as the liquid feed flow rate increased from 1.5 to 4.5 ml/h, while this change at 300 ℃ led to reduction of conversion from 96 to 90%. On the other hand, when temperature was increased from 255 to 290 ℃, the methanol conversion was increased from 68 to 93 in liquid flow rate of 1.5 ml/h, while increased from 55 to 85 in liquid flow rate of 4.5 ml/h.

Methanol conversion continuously increases when temperature increases. As discussed in previous work [27,30], Cu-SiO_2 catalyst has excellent selectivity to methanol reforming reaction and no CO forms in the proposed reaction mechanism for this catalyst or as by-product of reactants. However, when approaching the approximately complete conversion of methanol at high temperatures or at low feed flow rates, CO can be formed as a consecutive product through

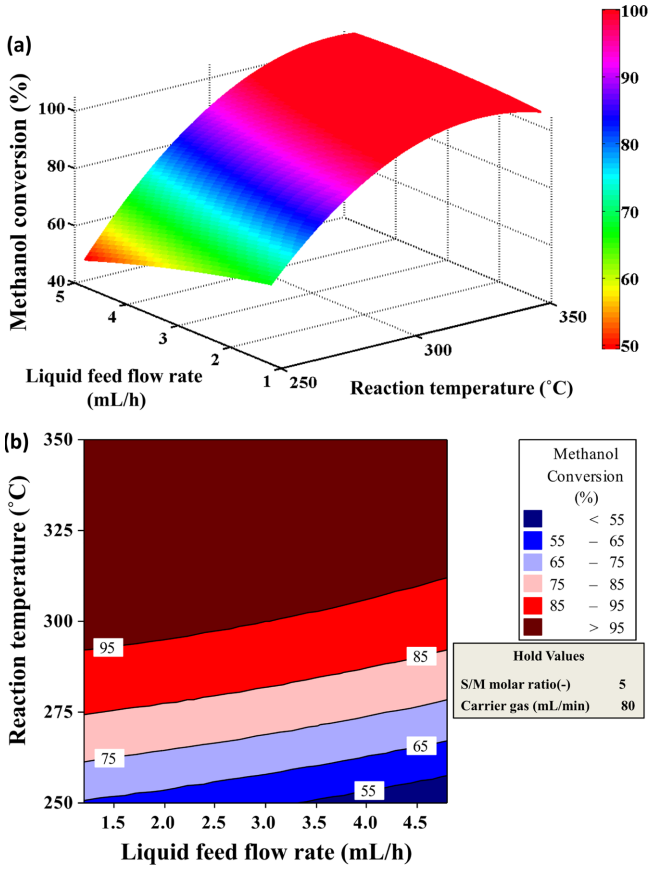

Fig. 3. (a) Response surface and (b) contour plots of the Methanol conversion (%) as a function of Liquid feed flow rate (mL/h) and Reaction temperature (℃) (Steam/Methanol molar ratio: 5 and Carrier gas flow (mL/min): 80).

the reverse water-gas shift reaction as a secondary reaction. Even if the reverse water-gas shift reaction occurs, the conversion of the methanol will be increased by temperature rising, because it consumes H_2 and CO_2 which are the products of methanol reforming.

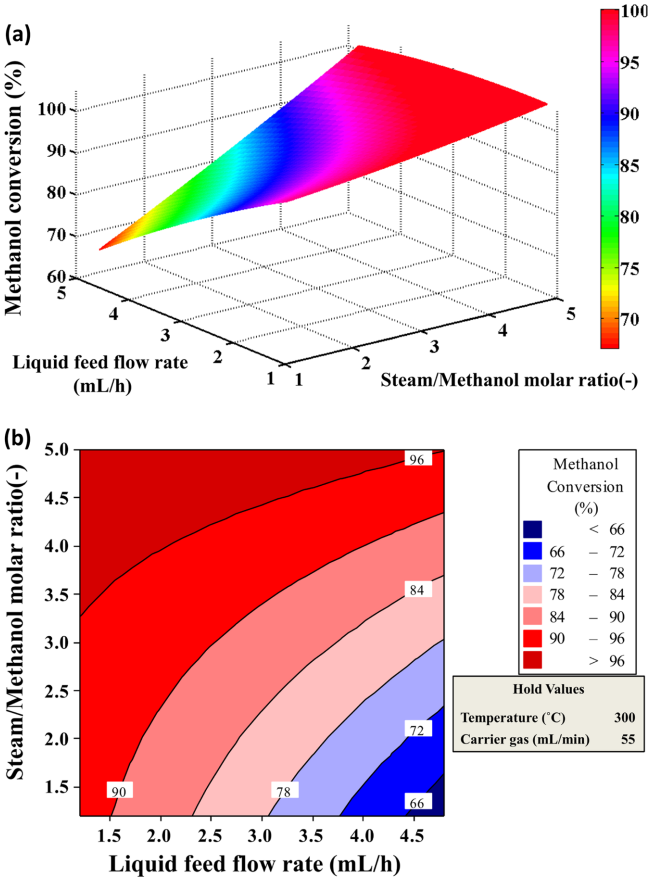

Fig. 4. (a) Response surface and (b) contour plots of the Methanol conversion (%) as a function of Liquid feed flow rate (mL/h) and Steam/Methanol molar ratio (Reaction temperature (℃): 300 and Carrier gas flow (mL/min): 55).

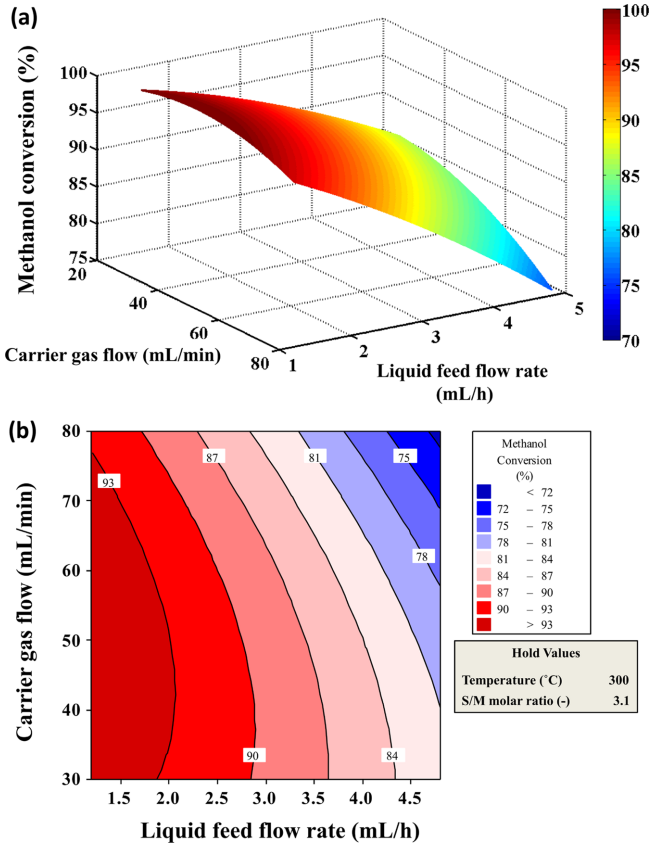

Fig. 5. (a) Response surface and (b) contour plots of the Methanol conversion (%) as a function of Liquid feed flow rate (mL/h) and Carrier gas flow (mL/min) (Reaction temperature (℃): 300, Steam/Methanol molar ratio: 3.1).

3-3-2. Effect of liquid feed flow rate and Steam/Methanol ratio on methanol conversion

As seen from Fig. 4, higher S/M ratio leads to higher methanol conversion. This result shows that the steam existence in the reaction surroundings improves the catalyst activity and leads to higher methanol conversion.

In a constant liquid flow rate, higher S/M ratio leads to higher methanol conversion. This result confirms the favorable effect of steam on the catalyst activity. Higher excess value of steam ensures higher conversion of limiting component.

The effect of the S/M ratio on the methanol conversion at higher feed flow rates is more significant. So, by increasing the S/M ratio from 1.5 to 4 in the feed flow rate of the 4.5ml/h the conversion is increased from about 67% to 88%, while in the feed flow rate of the 2 ml/h the conversion increased from about 89% to 96%.

Inversely, the feed flow rate effect is more significant at lower S/M ratios. So, increasing the feed flow rate from 1.5 ml/h to 4.5 ml/h at S/M=1.5 leads to methanol conversion decreasing from 91% to 67%, while at S/M=4 leads to methanol conversion decreasing from 97% to 88%. This result again can be related to the positive effect of water presence in the methanol reforming process. At higher S/M ratios, decreasing the retention time has less effect on the methanol conversion and the water presence prevents from the sharply reduction of MeOH conversion.

3-3-3. Effect of flow rates of liquid feed and carrier gas on Methanol conversion

Higher carrier gas flow lowers the residence time as well as the concentration of reactors within the reactor, thus, leads to lower conversion of methanol. Also, in the studied ranges of the liquid flow rate and carrier gas flow, the higher the liquid flow rate leads to the more influence of the carried gas flow rate on the conversion. By increasing the flow rate of carrier gas from 30 to 80 ml/min in the liquid flow rate of the 1.5 ml/h, the methanol conversion only decreased 3% (from 94% to 91%), while in the liquid flow rate of 4.5 ml/h the methanol conversion reduction was about 10% (83.5% to 74%). Lower feed flow rate in comparison with higher feed flow rate results in higher methanol conversion; therefore, increasing the methanol conversion through the same decreasing of the carrier gas flow rate will be harder in lower feed flow rates.

3-4. ANN Modelling results

ANN modeling was conducted using the experimental results (total 27 runs) reported in Table 2. So as to design the topology of the ANN, the number of neurons in the output and input layers is fixed

Table 5. Matrices of weights: W_1: weights between the input and the hidden layers; W_2: weights between the hidden and the output layers

Neuron	W_1				Bias	W_2	
	Variables					Neuron	weight
	Liquid feed flow rate	Reaction temperature	Steam/Methanol molar ratio	Carrier gas flow			
1	1.631	-4.778	-2.579	1.122	0.527	1	-7.521
2	2.595	-9.592	-13.878	6.819	2.379	2	1.323
						Bias	2.296

by the number of response and independent variables, respectively. As the main aspect to accomplish optimal network topology is the selection of the number of neurons in the hidden layer, the size of this layer is iteratively decided by altering the number of neurons to minimize the deviation of predictions from actual results [51]. For the optimum trained ANN, the biases and weight values between ANN layers are summarized in Table 5.

In the current study, the optimal ANN architecture comprises the reaction temperature (℃), liquid feed flow rate (mL/h), Carrier gas flow (mL/min) and S/M ratio (-) as the four inputs, two neurons in the hidden layer and methanol conversion (%) as an output, feed-forward back-propagation. Three layered neural network (BPNN) having the topology (4: 2: 1) was adopted in this work. Furthermore, the training algorithm involved was *trainlm* algorithm (Levenberg-Marquardt). During the training of network, the sigmoid transfer function predicted better results compared to other functions such as *purelin* and *tansig* transfer functions. Accordingly, the sigmoid transfer function was chosen to be the intention of the hidden and output layers. A representation of the optimized ANN architecture is apparent from Fig. 6. The back-propagation (BP) training algorithm, which was developed to provide a correlation between the output and the four inputs, can be undertaken using the experimental results made known in Table 2.

Fig. 7 illustrates regression plots (experiment vs. ANN predicted) using optimal 4 neurons in the hidden layer. As the regression coefficients (R^2) for the constructed ANN model and experimental responses are closely equal to 1, this has signified the importance of hidden layer neurons on the model efficiency (Fig. 7). Accordingly, higher values of R^2 of the ANN predicted for the training, validation and testing datasets put forward that the constructed ANN is accurately capable to predict the methanol conversions.

Due to proper utilization of the sigmoid transfer function for the output and hidden layers, Eq. (1) was used to normalize all the data of the experiments (Xi) to normalized values (xi) in a uniform range (0.1 to 0.9) [49].

Relative importance of each input variable can be calculated using the weight matrix [49]. The results are shown in Fig. 8. All chosen operation parameters strongly influence methanol conversion. Therefore, none of the studied variables can be ignored in analysis of the process. According to the findings, in methanol steam reforming in the presence of Cu-SiO_2 aerogel catalyst, the most effective parameter is reaction temperature with 44.55% relative importance. The relative importance of input parameters on the amount methanol steam reforming is as follows, which is in agreement with results of the BBD model: reaction temperature > steam/methanol molar ratio > liquid feed flow rate > carrier gas flow.

3-5. Comparison between the BBD and ANN models

Even though the RSM based BBD model offers several advantages, for instance, the capability to figure out the quadratic (second-order) effect of each response, to determine the interrelationships among factors and specify the optimal response with a rather small number of experiments [52], however, its proper utilization is restricted to correct determination of all factor ranges [49]. Unlike a BBD model, which is just suitable for quadratic approximations, ANNs, as alternative powerful tools for modelling non-linear multivariate systems, can be

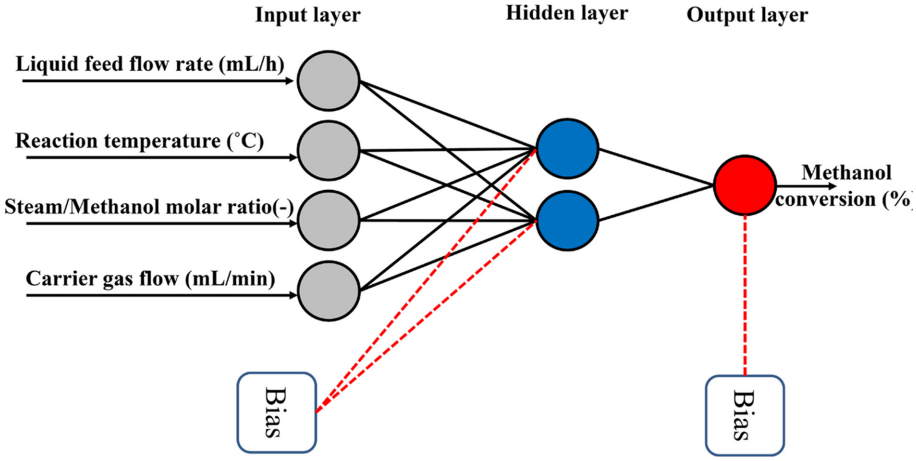

Fig. 6. The optimized structure of constructed ANN.

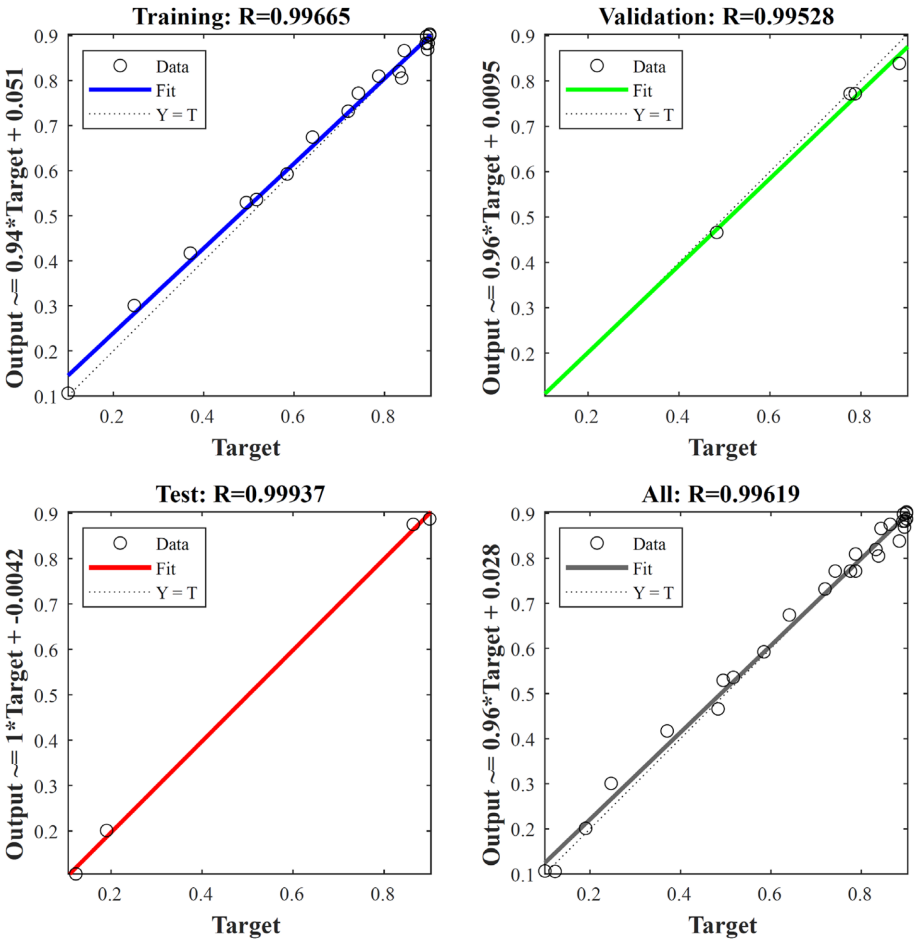

Fig. 7. Regression plots (experiment vs. ANN predicted) using 2 neurons in hidden layer.

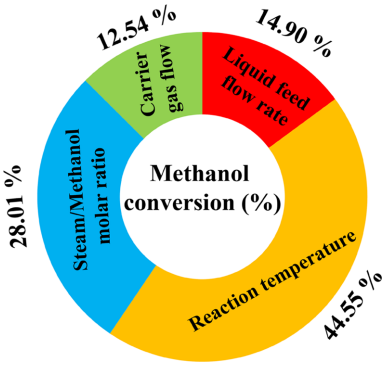

Fig. 8. Relative importance (%) of the input variables on the value of methanol conversion.

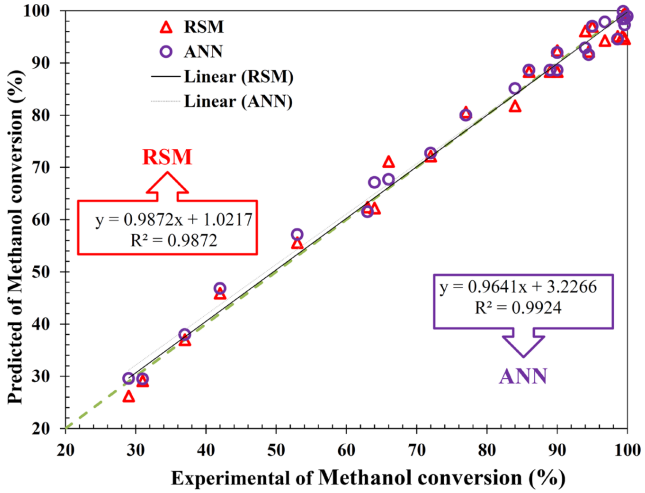

Fig. 9. Comparison between the predicted (BBD and ANN) values and the experimental results for methanol conversion (%).

used not only to approximate quadratic functions but also to estimate nearly all kinds of complex, non-linear functions.

The goodness of fit for the given models can be verified by comparing the experimental results of the methanol conversion in Table 2 and those predicted by the proposed RSM and ANN models. Fig. 9 represents a comparative parity plot of the predicted and actual results. The coefficient of determination (R^2 = 0.9872) for BBD and (R^2 = 0.9924) for ANN illustrates that the RSM and ANN based predictions are in excellent agreement with the experimentally observed consequences. This implies that 1.28% of the entire variation is not interpreted by the RSM model, whereas that of 0.76% is not described by the ANN model. Accordingly, the proposed models can be considered to perform well in data fitting and provide stable responses. However, compared to RSM, ANN model has a higher

Table 6. Comparison of between ANN and BBD

Parameters	RSM model	ANN model
Regression coefficient (R^2)	0.9872	0.9924
MAE	2.177	1.734
MSE	6.724	4.540
RMSE	2.593	2.131
Model developing	With interactions	Without interactions

predictive ability and accuracy on the basis of the R^2 value, being nearer to 1.0.

Apart from regression coefficient (R^2), the MAE, MSE and RMSE values observed for both models were determined to provide statistical indications of how accurate the model predictions can be. The MAE, MSE and RMSE for the RSM and ANN models were computed and summarized in Table 6. As indicated in Table 5, the MAE (2.177), MSE (6.724) and RSME (2.593) for the RSM model are greater than those (1.734, 4.540 and 2.131, respectively) for the ANN model, demonstrating that the ANN model has a greater modeling ability than the RSM model. It is noteworthy that the criteria given in Table 6 are calculated based on the real (non-normalized) data.

4. Conclusions

The current study was undertaken to model hydrogen production through methanol steam reforming. Our prime research objective set out to examine the effects and interaction effects of influential variables on performance of Cu-SiO_2 aerogel catalyst in methanol steam reforming. In this respect, particular focus was on the application of RSM based BBD approach to acquire a quadratic polynomial model and predict the amount of methanol conversion. Then, the BBD results were in comparison to ANN predictions with the aim of attaining the best modeling as well as powerful predictive tool for producing hydrogen. It can be also concluded that among the operating variables, the temperature is the most Influential parameter (56% importance) in methanol conversion. The proposed models were assessed based on the statistical criteria and both models seemed perfectly satisfactory. However, the results of the statistical indices indicated relative superiority of ANN compared to RSM in describing nonlinear behavior of the hydrogen production process.

References

1. Cai, F., Lu, P., Ibrahim, J. J., Fu, Y., Zhang, J. and Sun, Y., "Investigation of the Role of Nb on Pd−Zr−Zn Catalyst in Methanol Steam Reforming for Hydrogen Production," *International J. Hydrogen Energy*, **44**(23), 11717-11733(2019).
2. Ke, Y., Zhou, W., Chu, X., Yuan, D., Wan, S., Yu, W. and Liu, Y., "Porous Copper Fiber Sintered Felts with Surface Microchannels for Methanol Steam Reforming Microreactor for Hydrogen Production," *International J. Hydrogen Energy*, **44**(12), 5755-5765 (2019).
3. Liu, Y., Zhou, W., Chen, L., Lin, Y., Xuyang, C., Zheng, T. and Wan, S., "Optimal Design and Fabrication of Surface Microchannels on Copper Foam Catalyst Support in a Methanol Steam Reforming Microreactor," *Fuel*, **253**, 1545-1555(2019).
4. Ouyang, K., Wu, H. W., Huang, S. C. and Wu, S. J., "Optimum Parameter Design for Performance of Methanol Steam Reformer Combining Taguchi Method with Artificial Neural Network and Genetic Algorithm," *Energy*, **138**, 446-458(2017).
5. Perng, S.-W., Horng, R.-F. and Ku, H.-W., "Numerical Predictions of Design and Operating Parameters of Reformer on the Fuel Conversion and CO Production for the Steam Reforming of Methanol," *International J. Hydrogen Energy*, **38**(2), 840-852 (2013).
6. Tahay, P., Khani, Y., Jabari, M., Bahadoran, F., Safari, N. and Zamanian, A., "Synthesis of Cubic and Hexagonal $ZnTiO_3$ as Catalyst Support in Steam Reforming of Methanol: Study of Physical and Chemical Properties of Copper Catalysts on the H_2 and CO Selectivity and Coke Formation," *International J. Hydrogen Energy* (2020).
7. Fasanya, O. O., et al., "Copper Zinc Oxide Nanocatalysts Grown on Cordierite Substrate for Hydrogen Production Using Methanol Steam Reforming," *International J. Hydrogen Energy*, **44**(41), 22936-22946 (2019).
8. Phongboonchoo, Y., Thouchprasitchai, N. and Pongstabodee, S., "Hydrogen Production with a Low Carbon Monoxide Content via Methanol Steam Reforming over CuxCeyMgz/Al_2O_3 Catalysts: Optimization and Stability," *International J. Hydrogen Energy*, **42**(17), 12220-12235(2017).
9. Qing, S.-J., et al., "Catalytic Performance of Cu-Ni-Al Spinel for Methanol Steam Reforming to Hydrogen," *J. Fuel Chemistry and Technology*, **46**(10), 1210-1217(2018).
10. Sarafraz, M. M., et al., "Reforming of Methanol with Steam in a Micro-reactor with Cu–SiO_2 Porous Catalyst," *International J. Hydrogen Energy*, **44**(36), 19628-19639(2019).
11. Ribeirinha, P., et al., "Study of Different Designs of Methanol Steam Reformers: Experiment and Modeling," *International J. Hydrogen Energy*, **39**(35), 19970-19981(2014).
12. Shanmugam, V., et al., "Hydrogen Production over Highly Active Pt Based Catalyst Coatings by Steam Reforming of Methanol: Effect of Support and co-support," *International J. Hydrogen Energy*, **45**(3), 1658-1670(2020).
13. Tang, H.-Y., Greenwood, J. and Erickson, P., "Modeling of a Fixed-bed Copper-based Catalyst for Reforming Methanol: Steam and Autothermal Reformation," *International J. Hydrogen Energy*, **40**(25), 8034-8050(2015).
14. Herdem, M. S., Farhad, S. and Hamdullahpur, F., "Modeling and Parametric Study of a Methanol Reformate Gas-fueled HT-PEMFC System for Portable Power Generation Applications," *Energy Conversion and Management*, **101**, 19-29(2015).
15. Wan, Y., Zhou, Z. and Cheng, Z., "Hydrogen Production from Steam Reforming of Methanol over CuO/ZnO/Al_2O_3 Catalysts: Catalytic Performance and Kinetic Modeling," *Chinese J. Chemical Engineering*, **24**(9), 1186-1194(2016).
16. Vidal Vázquez, F., et al., "Reactor Design and Catalysts Testing for Hydrogen Production by Methanol Steam Reforming for Fuel Cells Applications," *International J. Hydrogen Energy*, **41**(2), 924-935(2016).

17. Wu, W., et al., "Design, Modeling, and Optimization of a Lightweight MeOH-to-H_2 Processor," *International J. Hydrogen Energy*, **43**(31), 14451-14465(2018).
18. Sari, A. and Sabziani, J., "Modeling and 3D-simulation of Hydrogen Production via Methanol Steam Reforming in Copper-coated Channels of a Mini Reformer," *J. Power Sources*, **352**, 64-76 (2017).
19. He, J., et al., "Cu Supported on ZnAl-LDHs Precursor Prepared by in-situ synthesis method on γ-Al_2O_3 as Catalytic Material with High Catalytic Activity for Methanol Steam Reforming," *International J. Hydrogen Energy*, **42**(15) 9930-9937(2017).
20. Ma, H., et al., "Two-dimensional Modeling of a Plant-scale Fixed-bed Reactor for Hydrogen Production from Methanol Steam Reforming," *International J. Hydrogen Energy*, **41**(38), 16932-16943(2016).
21. Chuang, C.-C., et al., "Optimal Design of An Experimental Methanol Fuel Reformer," *International J. Hydrogen Energy*, **33**(23), 7062-7073(2008).
22. Jang, J.-Y., Huang, Y.-X. and Cheng, C.-H., "The Effects of Geometric and Operating Conditions on the Hydrogen Production Performance of a Micro-methanol Steam Reformer," *Chemical Engineering Science*, **65**(20), 5495-5506(2010).
23. Zheng, T., et al., "Methanol Steam Reforming Performance Optimisation of Cylindrical Microreactor for Hydrogen Production Utilising Error Backpropagation and Genetic Algorithm," *Chemical Engineering J.*, **357**, 641-654(2019).
24. Purnama, H., Catalytic Study of Copper based Catalysts for Steam Reforming of Methanol, Ph.D. Dissertation, Technical University of Berlin, Berlin (2003).
25. Matsumura, Y. and H. Ishibe, "Selective Steam Reforming of Methanol over Silica-supported Copper Catalyst Prepared by Sol–gel Method," *Applied Catalysis B: Environmental*, **86**(3), 114-120(2009).
26. Takezawa, N., et al., "Steam Reforming of Methanol on Copper-silica Catalysts; Effect of Copper Loading and Calcination Temperature on the Reaction," *Applied Catalysis*, **4**(2), 127-134(1982).
27. Takezawa, N. and N. Iwasa, "Steam Reforming and Dehydrogenation of Methanol: Difference in the Catalytic Functions of Copper and Group VIII Metals," *Catalysis Today*, **36**(1), 45-56 (1997).
28. Tajrishi, O.Z., M. Taghizadeh, and A.D. Kiadehi, "Methanol Steam Reforming in a Microchannel Reactor by Zn-, Ce- and Zr-Modified Mesoporous Cu/SBA-15 Nanocatalyst," *International J. Hydrogen Energy*, **43**(31), 14103-14120(2018).
29. Yousefi Amiri, T. and J. Moghaddas, "Cogeled Copper–silica Aerogel as a Catalyst in Hydrogen Production from Methanol Steam Reforming," *International J. Hydrogen Energy*, **40**(3), 1472-1480(2015).
30. Amiri, T. Y. and Moghaddas, J., "Reaction Parameters Influence on the Catalytic Performance of Copper-silica Aerogel in the Methanol Steam Reforming," *J. Fuel Chemistry and Technology*, **44**(1), 84-90(2016).
31. Yousefi Amiri, T. and Moghaddas, J., "Performance Evaluation of Cu-SiO_2 Aerogel Catalyst in Methanol Steam Reforming," *Iranian J. Chemical Engineering*(IJChE), **11**(3), 37-44 (2014).
32. Yousefi Amiri, T., Moghaddas, J. and Rahmani Khajeh, S., "Silica Aerogel-supported Copper Catalyst Prepared Via Ambient Pressure Drying Process," *J. Sol-Gel Science and Technology*, **77**(3), 627-635(2016).
33. Chiu, Y.-J., et al., "Simulations of Hydrogen Production by Methanol Steam Reforming," *Energy Procedia*, **156**, 38-42(2019).
34. Kakelar, M. and S. Ebrahimi, "Up-scaling Application of Microbial Carbonate Precipitation: Optimization of Urease Production Using Response Surface Methodology and Injection Modification," *International J. Environmental Science and Technology*, **13**(11), 2619-2628(2016).
35. Karthic, P., et al., "Optimization of Biohydrogen Production by Enterobacter Species Using Artificial Neural Network and Response Surface Methodology," *J. Renewable and Sustainable Energy*, **5**(3), 033104(2013).
36. Chiu, Y.-J., et al., "Experimental Study on the Reaction Conditions of a Methanol Steam Reforming Process," *Energy Procedia*, **105**, 1622-1627(2017).
37. Liu, C.-H., Hwang, C.-F. and Liao, C.-C., "Medium Optimization for Glutathione Production by Saccharomyces Cerevisiae," *Process Biochemistry*, **34**(1), 17-23(1999).
38. He, L., Xu, Y. Q. and Zhang, X. H., "Medium Factor Optimization and Fermentation Kinetics for Phenazine-1-carboxylic Acid Production by Pseudomonas sp. M18G," *Biotechnology and Bioengineering*, **100**(2), 250-259(2008).
39. Wang, J. and Wan, W., "Optimization of Fermentative Hydrogen Production Process Using Genetic Algorithm Based on Neural Network and Response Surface Methodology," *International J. Hydrogen Energy*, **34**(1), 255-261(2009).
40. Nasr, N., et al., "Application of Artificial Neural Networks for Modeling of Biohydrogen Production," *International J. Hydrogen Energy*, **38**(8), 3189-3195(2013).
41. Adib, H., et al., "Modeling and Optimization of Fischer–Tropsch Synthesis in the Presence of Co (III)/Al_2O_3 Catalyst Using Artificial Neural Networks and Genetic Algorithm," *J. Natural Gas Science and Engineering*, **10**, 14-24(2013).
42. Dawson, C. W. and Wilby, R., "An Artificial Neural Network Approach to Rainfall-runoff Modelling," *Hydrological Sciences J.*, **43**(1), 47-66(1998).
43. Aghaeinejad-Meybodi, A., et al., "Modeling and Optimization of Antidepressant Drug Fluoxetine Removal in Aqueous Media by Ozone/H_2O_2 Process: Comparison of Central Composite Design and Artificial Neural Network Approaches," *J. Taiwan Institute Chemical Engineers*, **48**, 40-48(2015).
44. Asadzadeh, F., Maleki-Kakelar, M. and Shabani, F., "Predicting Cationic Exchange Capacity in Calcareous Soils of East-Azerbaijan Province, Northwest Iran," *Communications in Soil Science and Plant Analysis*, **50**(9), 1106-1116(2019).
45. Salehi, E., et al., "Data-based Modeling and Optimization of a Hybrid Column-adsorption/depth-filtration Process Using a Combined Intelligent Approach," *J. Cleaner Production*, **236**, 117664 (2019).
46. Khataee, A. R. and Kasiri, M. B., "Artificial Neural Networks Modeling of Contaminated Water Treatment Processes by Homogeneous and Heterogeneous Nanocatalysis," *J. Molecular Catalysis A: Chemical*, **331**(1), 86-100(2010).
47. Kumar, N. M., Ramasamy, R., and Manonmani, H., "Production and Optimization of l-asparaginase from Cladosporium sp. Using Agricultural Residues in Solid State Fermentation," *Indus-*

trial Crops and Products, **43**, 150-158(2013).
48. Maddipati, P., et al., "Ethanol Production from Syngas by Clostridium Strain P11 Using Corn Steep Liquor as a Nutrient Replacement to Yeast Extract," *Bioresource Technology*, **102**(11), 6494-6501(2011).
49. Aghaeinejad-Meybodi, A., et al., "Degradation of Fluoxetine Using Catalytic Ozonation in Aqueous Media in the Presence of Nano-γ-alumina Catalyst: Experimental, Modeling and Optimization Study," *Separation and Purification Technology*, **211**, 551-563(2019).
50. Aghaeinejad-Meybodi, A., et al., "Degradation of Antidepressant Drug Fluoxetine in Aqueous Media by Ozone/H_2O_2 System: Process Optimization Using Central Composite Design," *Environmental Technology*, **36**(12), 1477-1488(2015).
51. Baş, D. and Boyacı, İ. H., "Modeling and Optimization II: Comparison of Estimation Capabilities of Response Surface Methodology with Artificial Neural Networks in a Biochemical Reaction," *J. Food Engineering*, **78**(3), 846-854(2007).
52. Ghafari, E., Costa, H. and Júlio, E., "RSM-based Model to Predict the Performance of Self-compacting UHPC Reinforced with Hybrid Steel Micro-fibers," *Construction and Building Materials*, **66**, 375-383(2014).

Authors
Taher Yousefi Amiri: Assistant Professor, Department of Chemical Engineering, University of Zanjan, Zanjan, Iran; yousefiamiri@znu.ac.ir
Mahdi Maleki-Kakelar: Assistant Professor, Department of Chemical Engineering, University of Zanjan, Zanjan, Iran; mmaleki@znu.ac.ir
Abbas Aghaeinejad-Meybodi: Associated Professor, Department of Chemical Engineering, Urmia University, Urmia, Iran; a.aghaeinejad@urmia.ac.ir